

The Leidenfrost Point: Experimental Study and Assessment of Existing Models

J. D. Bernardin

Research Engineer,
Los Alamos National Laboratory

I. Mudawar

Professor and Director

Boiling and Two-Phase Flow Laboratory,
School of Mechanical Engineering,
Purdue University,
West Lafayette, IN 47907

This study presents a detailed and thorough parametric study of the Leidenfrost point (LFP), which serves as the temperature boundary between the transition and film boiling regimes. Sessile drop evaporation experiments were conducted with acetone, benzene, FC-72, and water on heated aluminum surfaces with either polished, particle blasted, or rough sanded finishes to observe the influential effects of fluid properties, surface roughness, and surface contamination on the LFP. A weak relationship between surface energies and the LFP was observed by performing droplet evaporation experiments with water on polished copper, nickel, and silver surfaces. Additional parameters which were investigated and found to have negligible influence on the LFP included liquid subcooling, liquid degassing, surface roughness on the polished level, and the presence of polishing paste residues. The accumulated LFP data of this study was used to assess several existing models which attempt to identify the mechanisms which govern the LFP. The disagreement between the experimental LFP values and those predicted by the various models suggests that an accurate and robust theoretical model which effectively captures the LFP mechanisms is currently unavailable.

1 Introduction

Recent demands for superior material properties and more efficient use of materials and production time are forcing manufacturers to develop intelligent processing techniques for enhanced process control in order to better dictate the end product. In the heat treatment and processing of metallic alloys, the desire to obtain parts of enhanced and uniform mechanical properties is requiring increased control over heat removal rates and enhanced temperature control. In particular, spray quenching has been shown (Bernardin and Mudawar, 1995) to be an effective means to control and enhance the cooling rates of heat treatable aluminum alloys. Rapid quenching is required to obtain high material strength, while uniform temperature control is necessary to reduce warping and deformation. In addition, the quench rate and material properties of aluminum alloys following solution heat treatment are dictated mainly by low heat flux, high-temperature film boiling spray heat transfer, and the Leidenfrost point (LFP) which forms the lower temperature limit of the film boiling regime (Bernardin, 1993). Thus, when quenching most aluminum alloys, it is desirable to traverse through the film boiling temperature range and get below the LFP as quickly as possible. Consequently, accurate knowledge of the Leidenfrost temperature is necessary if accurate and enhanced control of the quenching process and resulting material properties is desired.

A common technique used for determining the Leidenfrost temperature requires measuring evaporation times of liquid sessile droplets of a given initial volume over a range of surface temperatures to produce a droplet evaporation curve as shown in Fig. 1(b). The curve displays droplet evaporation lifetime versus surface temperature and exhibits the four distinct heat transfer regimes shown on the traditional pool boiling curve of Fig. 1(a). In the single-phase regime, characterized by long evaporation times, heat from the surface is conducted through the liquid film and is dissipated by evaporation at the liquid-gas interface. In the nucleate boiling regime, vapor bubble production and the corresponding

heat flux increase dramatically, thus decreasing the droplet lifetime. The upper limit of the nucleate boiling regime, known as critical heat flux (CHF), corresponds to a maximum heat flux and minimum drop lifetime. In the transition regime, a noncontinuous, insulating vapor layer develops beneath portions of the droplet, leading to reduced evaporation rates and increased drop lifetime. At the upper end of the transition boiling regime, referred to as the LFP, the vapor layer grows substantially to prevent any significant contact between the drop and surface and the droplet evaporation time reaches a maximum. At surface temperatures above the LFP, the droplet remains separated from the surface by a thin vapor layer through which heat is conducted.

Literature Review and Focus of Current Study. Table 1 displays the large variations in the Leidenfrost temperature for water which have been reported in the literature. The discrepancies in these reported values arise from differences in size of the liquid mass, method of liquid deposition, amount of liquid subcooling, solid thermal properties, surface material and finish, pressure, and presence of impurities. These parameters and their observed effects on the LFP are summarized in Table 2 along with the corresponding references.

While many of the LFP investigations have been qualitative in nature, several studies have reported various correlations for predicting the Leidenfrost temperature. One of the correlations most frequently referred to is a semi-empirical expression developed by Baumeister and Simon (1973). Adapting the superheat limit model of Spiegler et al. (1963), Baumeister and Simon included corrections to account for the thermal properties of the heated surface and wetting characteristics of the liquid-solid system, and arrived at the following semi-empirical expression:

$$T_{\text{leid, meas}} = T_f + \frac{0.844T_c \left\{ 1 - \exp \left(-0.016 \left[\frac{\left(\frac{\rho_s}{\sigma_f} \right)^{1.33}}{\sigma_f} \right]^{0.5} \right) \right\} - T_f}{\exp(3.066 \times 10^6 \beta) \operatorname{erfc}(1758 \sqrt{\beta})}, \quad (1)$$

where

Contributed by the Heat Transfer Division for publication in the JOURNAL OF HEAT TRANSFER. Manuscript received by the Heat Transfer Division, Feb. 2, 1998; revision received, Mar. 18, 1999. Keywords: Boiling, Droplet, Evaporation, Film, Heat Transfer, Two-Phase. Associate Technical Editor: D. Kaminski.

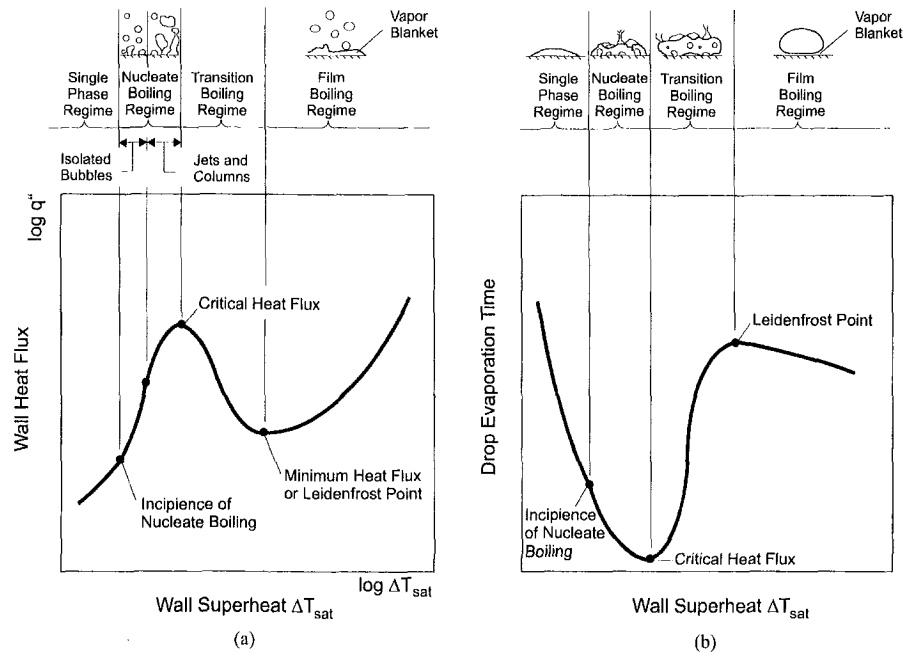


Fig. 1 (a) Boiling curve for a hot surface in a stagnant bath of liquid at saturation temperature and (b) sessile drop evaporation curve

$$\beta = \frac{1}{k_s \rho_s c_{p,s}} \quad (2)$$

The temperature generally measured and reported as the LFP corresponds to that of the solid in the near vicinity of the surface. To be more precise, it is better practice to associate the LFP with the temperature of the liquid-solid interface, which is often several degrees less than that measured within the solid. It is commonly accepted that during the initial stages of droplet-surface contact, the interface temperature between the liquid and solid is dictated by the thermal properties of the liquid and solid as well as by their initial temperatures. This interface temperature, T_i , is given by the solution to the one-dimensional energy equation with semi-infinite body boundary conditions (Eckert and Drake, 1972)

$$T_i = \frac{(k\rho c_p)_s^{0.5} T_{s,o} + (k\rho c_p)_f^{0.5} T_{f,o}}{(k\rho c_p)_s^{0.5} + (k\rho c_p)_f^{0.5}} \quad (3)$$

Nomenclature

A_t = atomic weight of surface material
 c_p = specific heat with constant pressure
 d = droplet diameter
 g = gravitational constant
 h = enthalpy
 h'_{fg} = modified latent heat of vaporization = $c_p(T_f - T_{sat}) + h_{fg}$
 J = vapor embryo formation rate per unit volume of liquid
 k = thermal conductivity
 k_b = Boltzmann constant
 M = molecular weight, constant
 m = mass of a single molecule
 N = number of liquid molecules per unit volume
 Na = Avogadro's number
 P = pressure

Q_a = heat of adsorption
 R = particular gas constant, drop, film, or bubble radius
 T = temperature
 u = droplet velocity
 v = specific volume, velocity

Greek Symbols

β = surface thermal parameter $(k\rho c_p)^{-1}$
 Γ = number of monolayer surface adsorption sites
 η = parameter for embryo formation rate equation
 λ = wavelength
 μ = dynamic viscosity
 θ = contact angle
 ρ = density
 σ = surface tension

τ_o = molecule residence time on surface

Subscripts

c = critical
 f = liquid
 fg = difference between liquid and vapor
 g = vapor
 i = interface
 $leid$ = Leidenfrost point
 mfb = minimum film boiling point
 o = initial
 r = reduced property
 s = surface, wall
 sat = saturation
 thn = thermodynamic homogeneous nucleation limit

The first objective of this study is to present previously developed models that attempt to describe the governing LFP mechanisms. Next, experimental LFP data for several different liquid-solid systems from the current study will be used to assess these models to display their weaknesses. Based upon lack of experimental validation and sound scientific arguments, a need for a correct and robust theoretical model that correctly captures the LFP mechanisms will be identified.

2 Previous LFP Models

This section discusses several of the most commonly proposed mechanisms for the LFP for droplets and the minimum film boiling point for pools of liquid. Table 3 contains a pictorial summary and corresponding correlations associated with the various models.

Hydrodynamic Instability Hypotheses. Several authors (Zuber, 1958; Berenson, 1961; Hosler and Westwater, 1962; Yao and

Table 1 Summary of Leidenfrost temperatures for water ($P = 101.3 \text{ kPa}$) as reported in the literature

Reference	$T_{leid} \text{ (}^\circ\text{C)}$	Surface Material	Notes
Blazkowska and Zakrzewska (1930)	157	Silver	
Borishansky and Kutateladze (1947) [†]	310 255	Graphite	$T_f = 20 \text{ }^\circ\text{C}$ $T_f = 85 \text{ }^\circ\text{C}$
Borishansky (1953) [†]	222 194 250 237	Brass Brass Copper Copper	$T_f = 19 \text{ }^\circ\text{C}$ $T_f = 89 \text{ }^\circ\text{C}$ $T_f = 20 \text{ }^\circ\text{C}$ $T_f = 85 \text{ }^\circ\text{C}$ $d_o = 4.5 \text{ mm}$
Tamura and Tanasawa (1959)	302	Stainless steel	
Gottfried (1962) [†]	285	Stainless steel	$T_f = 25 \text{ }^\circ\text{C}$ $3.7 < d_o < 4.3$
Betta (1963) ^{††}	245	Not given	$4.6 < d_o$
Lee (1965) ^{††}	280	Not given	$7.8 < d_o$
Godleski and Bell (1966)	320	Stainless steel	$T_{leid} = 264 \text{ }^\circ\text{C}$ for extended liquid masses and $161 \text{ }^\circ\text{C}$ for transient technique
Gottfried <i>et al.</i> (1966)	280	Stainless steel	
Kutateladze and Borishanski (1966)	250	Not given	
Patel and Bell (1966)	305	Stainless steel	$0.05 < V < 10 \text{ ml}$ extended masses
Baumeister <i>et al.</i> (1970)	515 305, 325 230, 235 >200 235 155 265 <184	Pyrex (3-4 rms) Stainless steel (3-4 rms) Brass (3-4 rms) Brass fresh polish (3-4 rms) Aluminum (3-4 rms) Alum. fresh pol. (3-4 rms) Aluminum (25 rms) Gold fresh polish	$d_o = 0.39 \text{ mm}$ $d_o = 0.39 \text{ \& } 2.25 \text{ mm}$ $d_o = 0.39 \text{ \& } 2.25 \text{ mm}$ $d_o = 2.25 \text{ mm}$ $d_o = 0.39 \text{ \& } 2.25 \text{ mm}$ $d_o = 0.39 \text{ mm}$ $d_o = 2.25 \text{ mm}$ $d_o = 2.25 \text{ mm}$
Emmerson (1975)	282 316 284	Stainless steel Monel Brass	LFP also given for pressures of 210, 315, 420, and 525 kPa
Xiong and Yuen (1991)	280-310	Stainless steel	

[†] As referenced from Patel and Bell (1966), ^{††} As referenced from Testa and Nicotra (1986)

Henry, 1978) have used a hydrodynamic stability theory by Taylor (1950) to describe the minimum film boiling temperature for pool boiling. Assuming potential flow and a sinusoidal disturbance between two fluids of different densities (the more dense on top), Taylor (1950) used a first-order perturbation analysis to show that gravity induced interfacial disturbances with wavelengths given by the following expression will be most likely to grow and disrupt the smooth horizontal interface:

$$\lambda_d = 2\pi \left[\frac{3\sigma_f}{g(\rho_f - \rho_g)} \right]^{1/2} \quad (4)$$

Berenson (1961) showed that the bubble spacing in film boiling was hydrodynamically controlled by a Taylor-type instability and that the presence of the corresponding vapor layer and bubble departure supported film boiling by keeping the liquid from contacting the heated surface. Berenson's analytical expression, Eq. (5), to predict the minimum film pool boiling temperature, T_{mfb} , coincides with the point at which vapor is not generated rapidly enough to sustain the Taylor waves at the liquid-vapor interface.

$$T_{mfb} = T_{sat} + 0.127 \frac{\rho_g h_{fg}}{k_g} \left[\frac{g(\rho_f - \rho_g)}{\rho_f + \rho_g} \right]^{2/3} \times \left[\frac{\sigma}{g(\rho_f - \rho_g)} \right]^{1/2} \left[\frac{\mu_g}{g(\rho_f - \rho_g)} \right]^{1/3} \quad (5)$$

Sakurai *et al.* (1982) and Groenveld (1982) showed that Berenson's model was only fair in predicting their minimum film boiling temperature data at low pressures and was in extreme error at high pressures.

Metastable Liquid—Homogeneous and Heterogeneous Nucleation Hypotheses. Yao and Henry (1978) and Sakurai *et al.* (1982) proposed that spontaneous bubble nucleation at the liquid-solid interface is the mechanism for the minimum pool film boiling point. Bubble nucleation can be either heterogeneous, in which the vapor bubbles are produced within cavities at a solid-liquid inter-

Table 2 Summary of the Influential LFP parameters

Parameter	Observations/References
Size of liquid mass	<ul style="list-style-type: none"> LFP independent of liquid mass size (Gottfried <i>et al.</i> 1966 and Patel and Bell, 1966). LFP increased with droplet volume (Nishio and Hirata, 1978).
Method of liquid deposition	<ul style="list-style-type: none"> LFP differed between steady state drop size technique using a pipet and the transient sessile drop technique (Godleski and Bell, 1966). LFP increased with droplet velocity (Patel and Bell, 1966; Yao and Cai, 1988; Klünzing <i>et al.</i>, 1993; and Labeish, 1994). LFP did not differ between sessile and impinging drops ($u_o < 5 \text{ m/s}$) (Bell, 1967 and Nishio and Hirata, 1978).
Liquid subcooling	<ul style="list-style-type: none"> Liquid subcooling had little effect on LFP for water on polished aluminum, brass, and stainless steel, but did cause an increased LFP on Pyrex (Baumeister <i>et al.</i> 1970). Subcooling increased drop lifetime but did not influence the LFP (Hiroyasu <i>et al.</i>, 1974). Subcooling raised the LFP for water and other fluids at high pressures where both sensible and latent heat exchange are significant (Emmerson and Snoek, 1978).
Solid thermal properties	<ul style="list-style-type: none"> LFP increases as solid thermal capacitance decreases (Patel and Bell, 1966; Baumeister <i>et al.</i>, 1970; and Nishio and Harata, 1978). Baumeister and Simon (1973) developed a LFP correlation accounts for solid thermal properties. LFP independent of solid thermal diffusivity (Bell, 1967 and Emmerson, 1975).
Surface conditions	<ul style="list-style-type: none"> Gottfried <i>et al.</i> (1966) estimated that the vapor layer beneath a film boiling sessile water drop was on the order of $10 \mu\text{m}$, which is on the same length scale as surface asperities on machine finished surfaces (Bernardin, 1993). Thus, rough surfaces in comparison to polished surfaces would be expected to require a higher LFP to support a thicker vapor layer to avoid liquid-solid contact for a sessile drop (Bradfield 1966). LFP increased as surface roughness and fouling increased (Baumeister <i>et al.</i>, 1970; Baumeister and Simon, 1973; and Nishio and Hirata, 1978). In contrast, Bell (1967) claimed that surface oxide films had a negligible effect on the LFP for droplets. LFP increased with increasing surface porosity (Avedisian and Koplik, 1987). LFP decreased with increased advancing contact angle in pool boiling (Kovalev, 1966; Unal <i>et al.</i>, 1992; and Labeish, 1994 and Ramilison and Lienhard, 1987).
Pressure	<ul style="list-style-type: none"> LFP increased with pressure for various fluids (Nikolayev <i>et al.</i>, 1974; Hiroyasu <i>et al.</i>, 1974; and Emmerson, 1975; Emmerson and Snoek, 1978) $(T_{leid} - T_{sat})$ found to remain constant for various pressures (Hiroyasu <i>et al.</i>, Emmerson, Nishio and Hirata, 1978, and Testa and Nicotra, 1986). Rhodes and Bell (1978) observed $(T_{leid} - T_{sat})$ for Freon-114 to be constant over a reduced pressure range of 0.125 to 0.350 and found it to decrease with increasing pressure above this range. Klimentko and Snytin (1990) reported similar findings for four inorganic fluids.

Table 3 Summary of proposed LFP models

Model	Pictorial Description	Relevant Correlations
Hydrodynamic Instability		Most dangerous wavelength: $\lambda_d = 2\pi \left[\frac{3\sigma_f}{g(\rho_f - \rho_g)} \right]^{1/2}$
Metastable liquid-mechanical stability		Mechanical stability condition: $\left(\frac{\partial P}{\partial v} \right)_T = 0$ Spinodal or liquid superheat limit: (using Van der Waals eqn.) $T_{thn} = 0.844 T_c$
Metastable liquid-kinetic stability		Homogeneous nucleation limit: $J = N_f \left(\frac{3\sigma}{\pi m} \right)^{0.5} \exp \left\{ \frac{-16\pi \sigma^3}{3k_b T_f [\eta P_{sat}(T_f) - P_f]^2} \right\}$ $\eta = \exp \left[\frac{v_f [P_f - P_{sat}(T_f)]}{R T_f} \right]$
Thermo-mechanical effect		Implicit energy balance for LFP: $h_g(T_g) - h_f(T_{leid}) = 0.5 \left[v_g(T_g) - v_f(T_{leid}) \right] \left[P_{sat}(T_{leid}) - P_{sat}(T_g) \right]$
Wettability - contact angle		Contact angle temperature dependence: $\cos(\theta) = 1 + C(T_{co} - T)^{\frac{a}{1-a}}$
Wettability - surface adsorption		Monolayer molecular surface coverage temperature dependence: $\frac{\Gamma}{\Gamma_o} = \frac{\exp\left(\frac{Q_a}{RT_f}\right)}{\left(\frac{2\pi MRT}{Na P_o}\right)^{0.5} \Gamma_o + \exp\left(\frac{Q_a}{RT_f}\right)}$

face as a result of the imperfect wetting of the liquid, or homogeneous, where the bubble nuclei are formed completely within the liquid due to density fluctuations over a duration of 10^{-9} to 10^{-8} s (Skrupov et al., 1980).

In the discussion that follows, the metastable state and related physics of homogeneous and heterogeneous nucleation are briefly presented. A more detailed and lengthier discussion of the subject can be found in Skripov (1974) and Carey (1992).

In classical thermodynamics, phase transitions for simple compressible substances are treated as quasi-equilibrium events at conditions corresponding to the saturation state. Between the saturated liquid and saturated vapor states exists a two-phase region where liquid and vapor coexist. Within this region, the temperature and pressure of the two phases must be constant, and the Gibbs function, chemical potential, and fugacity of each phase must be equal. In real-phase transformations, deviations from classical thermodynamics occur under nonequilibrium conditions, such as the superheating of a liquid above its boiling point. These non-equilibrium or metastable states are of practical interest and are important in determining limits or boundaries of real systems.

Shown on the pressure-volume diagram in the pictorial of Table 3 are the superheated liquid and supercooled vapor regions separated by an unstable region. The lines separating these regions are referred to as the liquid and vapor spinodals, which represent the maximum superheating and supercooling limits.

Two different approaches have been used in the literature to predict the superheat limit. The first, based on a mechanical stability condition described by Eberhart and Schnyders (1973) and Carey (1992) for a closed system containing a pure substance which is not in thermodynamic equilibrium, is given as

$$\left(\frac{\partial P}{\partial v} \right)_T < 0. \tag{6}$$

Along the portion of the isotherm between the spinodal lines of Fig. 2, the inequality $\partial p/\partial v > 0$ violates the mechanical stability criterion given by Eq. (6). For this reason, this area is referred to as the unstable region. In the metastable and stable regions, where $\partial p/\partial v < 0$, the liquid or vapor may remain in its form indefinitely. The spinodal limit, at which $\partial p/\partial v = 0$, represents the onset of instability.

Cubic equations of state such as Van der Waals (Spiegler et al., 1963), Himpan (Lienhard and Karimi, 1981), and Berthelot (Blander and Katz, 1975) possess the type of behavior within the vapor dome as discussed above and thus can be used to predict the spinodal limit. Van der Waals equation in terms of the reduced variables $P_r = P/P_c$, $T_r = T/T_c$, and $v_r = v/v_c$, which have been nondimensionalized with the corresponding critical point variables, can be written as

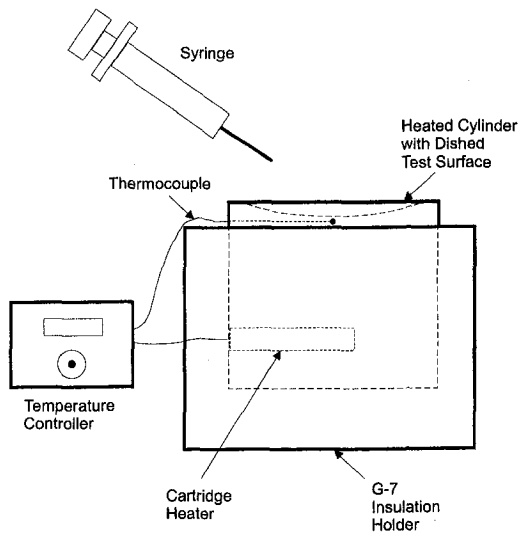


Fig. 2 Schematic diagram of sessile drop experimental apparatus

$$P_r = \frac{8T_r}{3v_r - 1} - \frac{3}{v_r^2} \quad (7)$$

Using this form of Van der Waals equation of state, the condition of mechanical stability given by Eq. (6), and the fact that $P_r \ll 1$ for most fluids at atmospheric conditions, the thermodynamic homogeneous nucleation temperature limit, T_{thn} , can be derived as (Spiegler et al., 1963)

$$T_{\text{thn}} = 0.844T_c, \quad (8)$$

where absolute temperature quantities are used. Modified forms of Eq. (8) using other equations of state and the success of these models in predicting the superheat limits of liquids are discussed in Carey (1992).

For fluids at higher pressures up to the critical point, Lienhard (1976) offered the following maximum superheat correlation:

$$T_{\text{thn}} = T_c \left[0.905 + 0.095 \left(\frac{T_{\text{sat}}}{T_c} \right)^8 \right], \quad (9)$$

where absolute temperatures are implied.

The second approach to describing the maximum liquid superheat temperature is referred to as the kinetic homogeneous nucleation theory, which bases the temperature and pressure dependence of bubble nucleation on molecular fluctuation probability. At and above saturation conditions, molecular fluctuations occur in such a way to cause a localized decrease in the liquid density, leading to the formation of vapor embryos. The fluctuation probability increases with temperature, and at the superheat temperature limit, the probability of a high bubble embryo formation rate is sufficient to transform the liquid to vapor.

By using conventional bubble nucleation theory, Carey showed how Eq. (10) could be derived to describe the rate of critical-size embryo formation, J , for a superheated liquid

$$J = N_f \left(\frac{3\sigma}{\pi m} \right)^{0.5} \exp \left\{ \frac{-16\pi\sigma^3}{3k_b T_f [\eta P_{\text{sat}}(T_f) - P_f]^2} \right\}, \quad (10)$$

where

$$\eta = \exp \left\{ \frac{v_f [P_f - P_{\text{sat}}(T_f)]}{RT_f} \right\}. \quad (11)$$

Slightly different assumptions have led to minor variations of Eq. (10) by several authors (Skripov, 1974; Blander and Katz, 1975; and Lienhard and Karimi, 1981).

The embryo formation rate given by Eq. (10) increases contin-

uously with temperature. However, because the exponential term has such a strong dependence on the liquid equilibrium temperature, T_f , there exists a small temperature range over which the embryo formation rate begins to increase in a drastic manner. It is within this temperature range that the critical embryo formation rate required to initiate homogeneous nucleation is defined with a corresponding value of T_f equal to the maximum superheat or kinetic homogeneous nucleation temperature. From experimental superheat data for a large variety of fluids at atmospheric pressure, Blander and Katz (1975) obtained a threshold value of $10^{12} \text{ m}^{-3} \text{ s}^{-1}$. Using this value for J , Eq. (10) can be solved iteratively for the maximum superheat temperature of a given liquid.

Carey (1992) showed how the development of Eq. (10) can be modified to account for the liquid contact angle, θ , and thus describe the heterogeneous nucleation rate of a liquid at a perfectly smooth surface:

$$J = \frac{N_f^{2/3} (1 + \cos \theta) \left(\frac{3F\sigma}{\pi m} \right)^{1/2} \exp \left\{ \frac{-16\pi F\sigma^3}{3k_b T_f [\eta P_{\text{sat}}(T_f) - P_f]^2} \right\}}{2F}, \quad (12)$$

where

$$F = \frac{2 + 3 \cos \theta - \cos^3 \theta}{4}. \quad (13)$$

The principle factor which is not accounted for in the homogeneous and heterogeneous nucleation models is the influence on the molecular interactions caused by the presence of the solid-liquid interface. Surface energies become influential and continuum fluid theories are not necessarily valid within 50 \AA of the interface. Gerwick and Yadigaroglu (1992) recognized that liquid molecular interactions at an interface will be quite different from the bulk liquid. Using statistical mechanics, they developed a modified equation of state for the liquid which was a function of the distance from the solid surface. This equation of state was used to predict the superheat limit of the liquid and thus the rewetting or Leidenfrost temperature of the surface.

Thermomechanical Effect Hypothesis. Schroeder-Richter and Bartsch (1990) refuted the superheated metastable hypothesis of Spiegler et al. (1963) and proposed that the liquid and vapor near the solid surface are in saturated states at different pressures. The authors used a nonequilibrium flow boiling model with conservation equations and appropriate boundary conditions across the liquid-vapor interface, along with assumptions that the liquid immediately in front of the interface is at the Leidenfrost temperature, and that the change in enthalpy during the evaporation is supplied solely by the mechanical energy of the depressurizing liquid to establish the following implicit equation for the Leidenfrost temperature:

$$h_g(T_g) - h_f(T_{\text{leid}}) = 0.5 [v_g(T_g) - v_f(T_{\text{leid}})] [p_{\text{sat}}(T_{\text{leid}}) - p_{\text{sat}}(T_g)]. \quad (14)$$

Using saturation tables and an iterative procedure, Eq. (14) can be solved for the LFP.

Wettability Hypotheses. It has been speculated by several researchers that the temperature dependence of the contact angle is influential in controlling the Leidenfrost phenomenon. In a fundamental study by Adamson (1972), a theoretical model was developed that related the molecular surface adsorption of a solid to the liquid-solid contact angle:

$$\cos \theta = 1 + C(T_{co} - T)^{b(\alpha - b)}, \quad (15)$$

where T_{co} represents a pseudo-critical temperature, or the temperature at which the contact angle goes to zero, C is an integration constant, and b and α are temperature-independent coefficients from a molecular force balance expression given by Adamson. It

is evident from Eq. (15) that the contact angle decreases with increasing temperature, a trend consistent with experimental findings.

Based upon the work of Adamson, Olek et al. (1988) presented a semi-theoretical analysis which suggests that the wetting temperature or LFP corresponds to a zero contact angle or perfect wetting. The authors suggested that at the temperature, T_{co} , where the contact angle goes to zero, the liquid drop spreads into a sufficiently thin film such that enough vapor can be generated to disjoin the film from the surface. Olek et al. were only able to provide experimental data for two water-nonmetallic solid systems with which to evaluate their model. Their comparison showed fair agreement between the predicted and measured temperature-dependent contact angle trends. However, they failed to provide Leidenfrost temperature data for the two surfaces.

Segev and Bankoff (1980) offered a more plausible explanation of the Leidenfrost phenomenon based on wetting characteristics. They proposed that wetting of a hot solid surface by a liquid is controlled by a microscopic precursor film which advances in front of the much thicker spreading liquid film. The presence of the thin film, which is required for the advancing and wetting of the remainder of the liquid, is controlled by the temperature-dependent surface adsorption characteristics. The precursor film thickness decreases with increasing temperature and drops off sharply as the temperature threshold (the LFP) is reached. Above this temperature, adsorption of the liquid molecules beyond a monolayer is no longer possible, and surface wetting cannot occur.

Segev and Bankoff based their model on the Langmuir adsorption isotherm

$$\frac{\Gamma}{\Gamma_o} = \frac{\exp\left(\frac{Q_a}{RT_i}\right)}{\left(\frac{(2\pi MRT)^{0.5}\Gamma_o}{N_a P \tau_o}\right) + \exp\left(\frac{Q_a}{RT_i}\right)} \quad (16)$$

which describes the fraction of total monolayer surface adsorption sites, Γ_o , occupied by foreign molecules in terms of the liquid-solid interface temperature, T_i , heat of adsorption, Q_a , and residence time of a molecule in the adsorbed state, τ_o . Segev and Bankoff claimed that the LFP corresponds to a surface monolayer coverage fraction of 0.9, and by using $\Gamma_o = 10^{19}$ molecules/m² and $\tau_o = 10^{-13}$ s, Eq. (16) can be solved explicitly for the surface temperature if the heat of adsorption of the fluid's vapor on the solid is known.

3 Experimental Apparatus and Procedure

The sessile drop apparatus shown in Fig. 2 was used to study the evaporation characteristics of droplets on a heated surface. In particular, the liquid/solid interface temperature corresponding to the Leidenfrost point was determined from droplet evaporation curves for a variety of operating conditions. The sessile drop facility consisted of an instrumented test heater module, temperature controller, and a syringe. The various working fluids included acetone, benzene, FC-72, an inert fluorocarbon produced by the 3M corporation, and distilled water. Several test heater modules were fabricated from either a solid aluminum or copper cylinder with a shallow concave surface designed to contain the liquid droplets during states of transition and film boiling. To investigate surface material effects on the LFP, several copper heater modules were also electroplated with either silver or nickel to a thickness of 0.025 mm. The heater module was mounted in an insulating shell formed from G-7 phenolic, which is capable of withstanding surface temperatures of 300°C for short durations. An Ogden Type 33 temperature controller, a Watlow 150 Watt cartridge heater, and a calibrated Chromel-Alumel (type K) thermocouple (calibrated accuracy = $\pm 0.2^\circ\text{C}$) located 2.5 mm beneath the center of the test surface were used to monitor and control the surface temperature. A finite element analysis and several thermocouple

measurements near the edge of the module were used to verify that the temperature distribution across the plane just beneath the surface was uniform and representative of the surface temperature. Three different surface finishes including polished, particle blasted, and rough sanded, with arithmetic average surface roughness values of 97, 970, and 2960 nm, respectively, were used in the study. A glass syringe with a 24-gauge hypodermic needle having a 0.58-mm (0.023-in.) outer diameter, was used to slowly dispense droplets of uniform diameter onto the test heater. A static force balance between gravity and surface tension dictated the nearly consistent droplet diameter for a given fluid. A high-speed Ektapro motion analyzer was used to verify that the slow droplet generation technique produced uniformly sized droplets within an error band of ten percent. Preliminary tests, performed with water and different diameter needles, revealed no dependence of the LFP on initial droplet size. This is consistent with findings reported by Gaotfried et al. (1966) and Patel and Bell (1966). Consequently, only one initial droplet diameter (fluid dependent) was used in this study.

For each test, single droplet evaporation times were recorded versus surface temperature over a temperature range encompassing the entire boiling spectrum for each particular fluid. The experiments began by dispensing a single drop from a syringe onto the center of the test surface at a temperature well within the film boiling regime from an approximate height of 1 cm. A manual digital stopwatch was used to record the time to the nearest tenth of a second for complete visual evaporation of the drop. To minimize timer (± 0.1 s) and initial droplet size (± 10 percent) errors, five evaporation times were recorded for each temperature increment and then averaged together. This procedure was performed for ten-degree centigrade surface temperature increments from a temperature within the fluid's film boiling regime down to the boiling incipience temperature, with finer two degree centigrade increments being made around the LFP. Each set of droplet evaporation data was used to generate a droplet evaporation curve, similar to the one displayed in Fig. 1(b), from which the LFP was identified by interpolation. The Leidenfrost temperature, or droplet/solid interface temperature corresponding to the LFP, was then determined with Eq. (3), using the measured surface temperature corresponding to the LFP.

The sources of experimental error in determining the Leidenfrost temperature included uncertainties in initial droplet size (± 10 percent), droplet evaporation time (± 0.1 s), and surface temperature measurement ($\pm 0.2^\circ\text{C}$). An additional error was imposed by the graphical LFP interpolation uncertainty caused by the 2°C gap between data points near the LFP on the droplet evaporation plots. The uncertainty in droplet evaporation time was deemed minimal since the accuracy of the timer was nearly two orders of magnitude smaller than typical droplet evaporation times near the LFP. The uncertainty in droplet size was minimized by taking the average evaporation time of five droplets at each data point. The temperature measurement uncertainty combined with the graphical LFP interpolation error created by the 2°C gap between data points, resulted in a total experimental uncertainty of 4.4°C . This was found to be consistent with reproducibility tests that revealed the LFP measurements were repeatable within $\pm 5^\circ\text{C}$.

An extensive database was required for identifying key influential parameters and to assess several analytical and theoretical models. Consequently, the experimental procedure was performed for four different test fluids with and without degassing, various degrees of liquid subcooling, four different surface materials, a variety of surface finishes, and different forms of surface contamination. To investigate the effect of surface impurities left behind from previous drops, two different tests were performed. In one case, the surface was wiped clean with a fine tissue between successive drops, and in the other case, the surface was left as is. More detailed operating conditions for the various tests are discussed with the experimental results.

Table 4 Leidenfrost temperatures for various fluids and aluminum surface conditions

Fluid	T_{leid} (°C)		
	Surface Finish		
	Polished	Particle Blasted	Rough Sanded
Acetone (wiped)	135 [130, 140, 133]	155 [160, 150]	160 [160, 160]
Acetone (unwiped)	185 [185, 183]	200 [195, 203]	178 [180, 173]
Benzene (wiped)	175	220	218
Benzene (unwiped)	180	215	215
FC-72 (wiped)	90	110	120
FC-72 (unwiped)	115	110	120
Water (wiped)	171 [175, 180, 160, 170]	250 [250, 250]	263 [260, 263]
Water (unwiped)	225 [220, 230]	280 [280, 280]	263 [260, 263]

4 Experimental Results and Discussion

In the discussions that follow, the reported empirical Leidenfrost temperatures correspond to measured surface temperatures at the LFP. However, in the evaluations of the LFP models (Table 6), both the empirical Leidenfrost temperatures and adjusted LFP values (using Eq. (3) to account for the liquid/solid interface) are presented.

Table 4 presents the LFP data for acetone, benzene, FC-72, and distilled water on three different aluminum surface finishes for both wiped and unwiped conditions between successive drops. The average LFP values are displayed with large text in Table 4 while the small text in brackets indicates Leidenfrost temperatures from individual runs when more than one test was performed for a single set of operating conditions. The focus of this experimental data was to study the effects of fluid properties, surface roughness, and surface contamination on the LFP.

The Leidenfrost temperature data of Table 4 indicate the following general trends:

Effect of Surface Roughness: For all test fluids, polished surfaces had significantly lower Leidenfrost temperatures than particle blasted and rough sanded surfaces. The surface roughness dependence of the Leidenfrost temperature is speculated to be related to intermittent liquid-solid contact caused by surface aspirates poking through the thin vapor layer, which, as reported by Labeish (1994), is on the order of 1 μm . As the surface roughness increases, a thicker vapor layer, and hence a higher surface temperature, is required to keep the liquid separated from the solid surface. This effect would be expected to taper off as surface roughness increases, which is observed in the similar Leidenfrost temperatures for the particle blasted and rough sanded surfaces.

Effect of Surface Contamination: A wiped surface generally had a considerably lower Leidenfrost temperature than an unwiped surface. This was most evident for the polished surface and to a lesser degree for the particle blasted and rough sanded surfaces.

The surface deposits left from previous drops tended to serve as vapor bubble nucleation sources when making contact with newly deposited drops, much in the same way as the surface aspirates acted on the rougher surfaces. With deposits present, a higher surface temperature was required to sustain film boiling. This finding is consistent with those of Baumeister et al. (1970) who found that the Leidenfrost temperature for water on a freshly polished aluminum surface was 155°C, 70°C less than that of a conventional contaminated surface. It is intuitively obvious that surface contamination from previous drops will act to increase the roughness on a polished surface to a much larger degree than for an initially much rougher surface. This explains why the Leidenfrost temperature for a polished surface is highly influenced by deposits while the rougher surfaces are not.

Table 5 presents Leidenfrost temperature data for water and a variety of polished surface materials. The numbers in large text indicate average LFP temperature values while the numbers in small text and brackets indicate single experimental data points. The accuracy and sensitivity of the measurements resulted in a $\pm 15^\circ\text{C}$ band around the average Leidenfrost temperatures tabulated herein. The focus of this portion of the study was to investigate the influences of surface material, surface contamination from polishing pastes, surface roughness on the polished level, liquid subcooling, and liquid degassing on the LFP.

Effect of Surface Material and Polishing Paste Residue: Leidenfrost temperature values were obtained for water on polished aluminum, silver, nickel, and copper. The average Leidenfrost temperature is nearly identical for the aluminum, silver, and nickel surfaces but is significantly higher for the copper surface. The higher LFP value of the copper surface is speculated to be the result of surface roughening which accompanied large amounts of surface oxidation during heating. Jeschar et al. (1984) also reported a higher Leidenfrost temperature for copper compared to nickel and, as in this study, attributed this to roughening of the copper test piece by heavy oxidation. Labeish (1994) reported

Table 5 Measured Leidenfrost temperatures for water on polished surfaces

Surface	T_{leid} (°C)	Notes
Aluminum	170 [170]	• Study: material effect • Surface: polished with 45, 30, 15, 9, 6, & 3 micron diamond paste and chemically cleaned
Silver	176 [185 170 / 190 160]	• Study: material effect • Surface: polished with 45, 30, 15, 9, 6, & 3 micron diamond paste, silver plated, polished with Simichrome, wiped with acetone, oxidized upon heating
Nickel	173 [173 / 170]	• Study: material effect • Surface: polished with 45, 30, 15, 9, 6, & 3 micron diamond paste, nickel plated, wiped with acetone, no apparent oxidation
Copper	198 [185 200 / 210]	• Study: material effect • Surface: polished with 45, 30, 15, 9, 6, & 3 micron diamond paste and chemically cleaned, heavy oxidation upon heating surface
Nickel	181 [180 190 / 175 190 / 170]	• Study: material effect • Surface: polished with Simichrome, nickel plated, wiped with acetone, no apparent oxidation
Copper	193 [193 / 190]	• Study: material effect • Surface: polished with Simichrome paste, heavy oxidation upon heating surface
Aluminum	175 [170 173 / 180]	• Study: roughness effect • Surface Prep.: polished with 45 micron paste
Aluminum	181 [190 180 / 190 165]	• Study: roughness effect • Surface: polished with 45, 30, & 15 micron diamond paste
Aluminum	185 [180 / 190]	• Study: roughness effect • Surface: polished with 45, 30, 15, 9, 6, & 3 micron diamond paste
Aluminum	171 [175 160 / 180 170]	• Study: roughness effect • Surface: polished w/ 45, 30, 15, 9, 6, & 3 micron diamond paste then with Simichrome paste
Aluminum	178 [190 / 165]	• Study: degassing effects (water degassed) • Surface: polished with 9, 6, & 3 micron diamond paste and chemically cleaned
Aluminum	175	• Study: subcooling effect ($T_f = 90$ °C) • Surface: polished with 45, 30, 15, 9, 6, & 3 micron diamond paste and chemically cleaned
Aluminum	170	• Study: subcooling effect ($T_f = 60$ °C) • Surface: polished with 45, 30, 15, 9, 6, & 3 micron diamond paste and chemically cleaned
Aluminum	160	• Study: polishing paste effect • Surface: polished with Simichrome, then soaked & wiped with acetone

theoretical rewetting wall temperatures for smooth surfaces of different materials wetted by water drops. Accounting for surface thermal properties and neglecting surface effects, nearly identical rewetting temperatures of 270, 282, and 292°C were predicted for copper, nickel, and carbon steel, respectively. These predictions, while higher in absolute value than those reported in this study, indicate a relative insensitivity of the LFP to surface chemistry effects.

As the data of Table 5 indicates, no significant difference was observed in the Leidenfrost temperatures of polished aluminum

samples with the following surface finish preparations: polished with Simichrome paste; polished with Simichrome paste followed by soaking and wiping with acetone to remove the paste residue; and, polished with an array of diamond compounds followed by an acid bath chemical cleaning. The lack of variability in the LFP values for these three surfaces suggests that the polishing paste residue has little influence on the LFP.

Effect of Surface Roughness on the Polished Level: Average Leidenfrost temperatures for water on aluminum surfaces polished with different grades of diamond polishing compound all fell within a 15°C band, thus indicating no significant dependence of the LFP on surface roughness on the polished level.

Effect of Liquid Subcooling: For identical surface conditions, water liquid subcoolings of 10, 40, and 80°C resulted in Leidenfrost temperatures of 170, 170, and 175°C, respectively. The lack of sensitivity of the LFP on liquid subcooling results because the small amount of liquid contained in a single droplet, regardless of initial temperature, is rapidly heated to near saturated conditions when placed on the surface. This finding was also reported by Hiroyasu et al. (1974) and Grissom and Wierum (1981).

Effect of Liquid Degassing: Table 5 lists average Leidenfrost temperatures of 170°C and 178°C for nondegassed and degassed water, respectively, on a polished aluminum surface. Negligible differences of less than five percent were observed between nondegassed and degassed Leidenfrost temperatures for acetone and FC-72 on polished aluminum as well. Clearly, the effect of air and other non-condensable gases within the liquid on the LFP is minimal.

5 Assessment of Models

As mentioned previously, the temperature generally measured and reported as the LFP corresponds to that of the solid in the near vicinity of the surface. However, boiling is an interfacial phenomenon, and thus it is better practice to associate the LFP with the temperature of the liquid-solid interface. In the model assessments that follow, both the empirical Leidenfrost temperatures measured within the solid, and adjusted LFP values (using Eq. (3) to account for the liquid/solid interface) are presented in Table 6 for comparison.

Evaluation of Instability Models. To investigate whether or not a Taylor-type instability could control the Leidenfrost phenomenon, a length scale comparison can be made between the droplet diameter and the Taylor most dangerous interfacial wavelength, λ_d . For Benzene, FC-72, and water the corresponding values of λ_d are 17.7, 8.4, and 27.3 mm, respectively. These wavelengths are of the same order or larger than typical droplet diameters, which indicates that the Taylor interfacial instability, while possibly suitable for pool boiling analysis, does not lend itself to isolated

Table 6 Comparison of various Leidenfrost temperature (°C) models to experimental data for a polished aluminum surface

Fluid	Measured Leidenfrost temperature (°C)	Corrected liquid/solid interface Leidenfrost temperature (eqn. (3))	Berenson (1961) hydrodynamic model	Thermodynamic homogen. nucleation limit temperature	Kinetic homogen. nucleation limit temperature	Baumister and Simon (1973) correlation	Schroeder-Richter and Bartsch (1990) thermo-mechanical model
Acetone	134	132	152	156	198	130	‡
Benzene	175	172	140	201	239	171	180
Water	170	162	152	273	310	156	221
FC-72	90	89	‡	106	144	102	116

‡ Fluid properties unavailable to evaluate model.

boiling drops. Table 6 compares predictions for T_{leid} , using Berenson's (1961) model for T_{mb} (Eq. (5)) to experimentally measured sessile drop Leidenfrost temperatures for several of the fluids used in this study. The predictions show significant error for acetone and benzene and give only satisfactory results for water.

Evaluation of Metastable Liquid Models. Two theoretical models, the thermodynamic or mechanical stability model and the kinetic homogeneous nucleation model, have been developed using entirely different approaches to predict the maximum superheat temperature of liquids. However, attempting to use these models to predict the Leidenfrost temperature for sessile drops has not met reasonable success.

The Leidenfrost point correlation of Baumeister and Simon (1973) contains two sources of concern. First, in developing a conduction model to account for a decrease in the surface temperature at liquid-solid contact, the authors fail to explain how they arrived at the chosen value of an average heat transfer coefficient. Second and most importantly, Baumeister and Simon introduce a surface energy correction factor to the superheat model of Spiegler et al. While this factor leads to a correlation which successfully fits the data, the results may be deceiving in that they suggest that homogeneous nucleation, around which the correlation is constructed, is the mechanism governing the Leidenfrost phenomenon, when in fact, it may not be.

Experimental Leidenfrost temperatures for various liquids on a polished aluminum surface from the current study are compared to thermodynamic and kinetic superheat limits as well as the correlation of Baumeister and Simon (1973) in Table 6. All predictions were made with absolute temperature quantities and then converted to degrees Celsius. For the theoretical metastable liquid models, the superheat limits are considerably higher than the measured Leidenfrost temperatures for all fluids tested, consistent with the results of Spiegler et al. (1963). The semi-empirical correlation by Baumeister and Simon agrees quite well with the experimental data of the present study, but as previously mentioned, it fails to accurately model the physics governing the process. Obviously, superheat criteria alone do not accurately describe the Leidenfrost phenomenon for sessile drops on a heated surface.

While elegant, the modified equation of state and homogeneous nucleation model of Gerwick and Yadigaroglu (1992) involved several assumptions which severely limit its applicability and accuracy. First, a simple hard-sphere potential interaction model using London dispersion forces was used to describe the molecular interactions. This limits the model's applicability to nonpolar liquids, since liquids such as water, with highly polar hydrogen bonding forces, would not lend themselves to such modeling with any high degree of accuracy. Second, a parameter describing the strength of the wall-fluid interactions was stated to be unknown for most practical applications. Consequently, a simplified model which related this parameter to the contact angle was employed. The major argument against this simplification is that the contact angle is typically measured over a distance which is at least six orders of magnitude larger than the thickness of the fluid layer influenced by the presence of the solid surface. In fact, Adamson (1982) has hypothesized that the microscopic contact angle at the leading edge of the liquid film, which is on the order of several molecular diameters in thickness, is significantly smaller than the macroscopic contact angle commonly reported. In addition, the contact angle is highly influenced by surface roughness and impurities (Miller and Neogi, 1985; Bernardin et al., 1997), making it a highly undefined variable.

Evaluation of Nonequilibrium Model. Table 6 compares Leidenfrost temperatures predicted by Eq. (14) to experimentally measured values for several different fluids. The prediction for Benzene is quite good, while that for FC-72 is satisfactory, and the estimate for water is extremely poor.

Several problems exist in the development of Eq. (14) and its application to predicting the Leidenfrost temperature for droplets. First, the original model was constructed to emulate a vertical

dry-out flow boiling situation, a condition far from that of a sessile or impinging droplet. Next, and more importantly, the concept of saturated states at different pressures for the liquid and vapor rather than metastable superheating of the liquid at constant pressure is unsupported. Metastable states for fluids have been frequently observed (Avedisian, 1982; Shepherd and Sturtevant, 1982; McCann et al., 1989) and the physics of such nonequilibrium states have been well documented (Eberhart and Schnyders, 1973; Skripov, 1974; Lienhard and Karimi, 1978; Carey, 1992). In fact, liquid superheating forms the entire well established basis for bubble nucleation theory in boiling (Han and Griffith, 1965; Blander et al., 1971).

Evaluation of Wettability Models. The reasoning behind the contact angle model of Olek et al. (1988) appears unrealistic. In addition, the implicit equation for the LFP is difficult to verify since the required coefficients are only available for a few liquid-solid systems for which no Leidenfrost temperature data exists. The temperature-dependent contact angle measurements found by Bernardin and Mudawar (1997) for water on aluminum show little indication of a zero contact angle condition acting as the Leidenfrost point mechanism. Also in contrast to the model of Olek et al., nearly identical Leidenfrost temperatures were obtained in this study for two identically polished aluminum surfaces, one of which was left with a polishing paste residue, and the other which was chemically cleaned. Also, nearly identical Leidenfrost temperatures were obtained for aluminum, silver, and nickel surfaces, all of which have different wetting characteristics. The contact angle depends to such a large extent on the surface conditions (roughness, contamination, adsorption), as well as on liquid velocity and direction, it is a difficult parameter to characterize and effectively utilize. Thus it can be concluded that while surface wetting, as measured by the contact angle, may play a role in boiling heat transfer, it is not the controlling LFP mechanism.

The surface adsorption hypothesis of Segev and Bankoff (1980) is very difficult to verify for a liquid-surface combination because it requires the corresponding heat of adsorption of the fluid's vapor on the solid surface. Correct knowledge of the chemical makeup of a solid surface is very difficult to obtain. The presence of oxide layers or adsorbed layers of grease and other impurities changes the surface chemistry considerably. In addition, the experimental data of this study tends to disprove the hypothesis proposed by Segev and Bankoff. Using heat of adsorption for water vapor on aluminum oxide (McCormick and Westwater, 1965) and nickel oxide (Matsuda et al., 1992), Eq. (16) predicts Leidenfrost temperatures of 162 and 425°C for saturated water on aluminum and nickel, respectively. The predicted LFP value for the aluminum surface agrees reasonably well with the corresponding experimental value of 170°C, however, the model fails miserably for the nickel surface which had an experimental Leidenfrost temperature of 175°C. Segev and Bankoff's model suggests that the LFP for an aluminum surface possessing a polishing paste residue would be significantly different from an identically polished surface without the residue, a trend not observed in the experimental data of this study.

6 Conclusions

Sessile drop evaporation experiments were performed for a wide variety of operating conditions to establish a large LFP data base for identifying key influential parameters and assessing existing LFP models. From the experimental results, several key conclusions concerning the influential LFP parameters can be drawn.

- Liquid subcooling, the presence of dissolved gasses, and surface roughness on the polished level do not significantly influence the Leidenfrost temperature.
- Surface thermal properties will act to control the interface and hence Leidenfrost temperature. However, aside from thermal properties, the LFP is relatively insensitive to surface material as far as surface energies and wetting characteristics are concerned.
- Surface roughness, beyond that on the polished level, appears to

be a dominant parameter in controlling the Leidenfrost behavior. The data indicate, that for a given fluid, a polished surface possesses a relatively low Leidenfrost temperature in comparison to a particle blasted or rough sanded surface. In addition, surface impurities or deposits act to increase the relative surface roughness and the corresponding Leidenfrost temperature.

Sound arguments supported by experimental data were used to assess several hypothetical models of the LFP mechanism. These models were shown to lack robustness and were ineffective in predicting the Leidenfrost temperature. A model which successfully captures the Leidenfrost mechanism is currently being developed to account for several parameters which were found to actively influence the LFP in both previous investigations and the current study. These parameters include thermal properties of the solid, thermal and thermodynamic properties of the liquid, solid surface structure, pressure, and droplet impact velocity.

References

- Adamson, A. W., 1972, "Potential Distortion Model for Contact Angle and Spreading II. Temperature Dependent Effects," *J. Colloid Interface Sci.*, Vol. 44, pp. 273–281.
- Adamson, A. W., 1982, *Physical Chemistry of Surfaces*, John Wiley and Sons, Inc., New York.
- Avedisian, C. T., 1982, "Effect of Pressure on Bubble Growth Within Liquid Droplets at the Superheat Limit," *ASME JOURNAL OF HEAT TRANSFER*, Vol. 104, pp. 750–757.
- Avedisian, C. T., and Koplik, J., 1987, "Leidenfrost Boiling of Methanol Droplets on Hot Porous Ceramic Surfaces," *Int. J. Heat Mass Transfer*, Vol. 30, pp. 379–393.
- Baumeister, K. J., Henry, R. E., and Simon, F. F., 1970, "Role of the Surface in the Measurement of the Leidenfrost Temperature," *Augmentation of Convective Heat and Mass Transfer*, A. E. Bergles and R. L. Webb, eds., ASME, New York, pp. 91–101.
- Baumeister, K. J., and Simon, F. F., 1973, "Leidenfrost Temperature—Its Correlation for Liquid Metals, Cryogenics, Hydrocarbons, and Water," *ASME JOURNAL OF HEAT TRANSFER*, Vol. 95, pp. 166–173.
- Bell, K. J., 1967, "The Leidenfrost Phenomenon: A Survey," *Chem. Eng. Prog. Symposium Series*, Vol. 63, AIChE, New York, pp. 73–82.
- Berenson, P. J., 1961, "Film Boiling Heat Transfer from a Horizontal Surface," *ASME JOURNAL OF HEAT TRANSFER*, Vol. 83, pp. 351–358.
- Bernardin, J. D., 1993, *Intelligent Heat Treatment of Aluminum Alloys: Material, Surface Roughness, and Droplet-Surface Interaction Characteristics*, Masters thesis, Purdue University, West Lafayette, Indiana, IN.
- Bernardin, J. D., and Mudawar, I., 1995, "Validation of the Quench Factor Technique in Predicting Hardness in Heat Treatable Aluminum Alloys," *Int. J. Heat Mass Transfer*, Vol. 38, pp. 863–873.
- Bernardin, J. D., Mudawar, I., and Franses, E. I., 1997, "Contact Angle Temperature Dependence for Water Droplets on Practical Aluminum Surfaces," *Int. J. Heat Mass Transfer*, Vol. 40, pp. 1017–1033.
- Blander, M., Hengstenberg, D., and Katz, J. L., 1971, "Bubble Nucleation in *n*-Pentane, *n*-Hexane, *n*-Heptane + Hexadecane Mixtures, and Water," *J. Phys. Chem.*, Vol. 75, pp. 3613–3619.
- Blander, M., and Katz, J. L., 1975, "Bubble Nucleation in Liquids," *Amer. Inst. Chem. Eng. J.*, Vol. 21, pp. 833–848.
- Blaszkowska-Zakrzewska, H., 1930, "Rate of Evaporation of Liquids from a Heated Metallic Surface," *Bulletin International de l'Academie Polonaise*, Vol. 4a–5a, pp. 188–190.
- Bradfield, W. S., 1966, "Liquid-Solid Contact in Stable Film Boiling," *I & E C Fundamentals*, Vol. 5, pp. 200–204.
- Carey, V. P., 1992, *Liquid-Vapor Phase Change Phenomena: An Introduction to the Thermophysics of Vaporization and Condensation Processes in Heat Transfer Equipment*, Hemisphere, New York.
- Eberhart, J. G., and Schnyders, H. C., 1973, "Application of the Mechanical Stability Condition to the Prediction of the Limit of Superheat for Normal Alkanes, Ether, and Water," *J. Phys. Chem.*, Vol. 77, pp. 2730–2736.
- Eckert, E. R. G., and Drake, Jr., R. M., 1972, *Analysis of Heat and Mass Transfer*, McGraw-Hill, New York.
- Emmerson, G. S., 1975, "The Effect of Pressure and Surface Material on the Leidenfrost Point of Discrete Drops of Water," *Int. J. Heat Mass Transfer*, Vol. 18, pp. 381–386.
- Emmerson, G. S., and Snoek, C. W., 1978, "The Effect of Pressure on the Leidenfrost Point of Discrete Drops of Water and Freon on a Brass Surface," *Int. J. Heat Mass Transfer*, Vol. 21, pp. 1081–1086.
- Gerweck, V., and Yadigaroglu, G., 1992, "A Local Equation of State for a Fluid in the Presence of a Wall and its Application to Rewetting," *Int. J. Heat Mass Transfer*, Vol. 35, pp. 1823–1832.
- Godleski, E. S., and Bell, K. J., 1966, "The Leidenfrost Phenomenon for Binary Liquid Solutions," *Third International Heat Transfer Conference*, Vol. 4, Chicago, IL, AIChE, New York, pp. 51–58.
- Gottfried, B. S., Lee, C. J., and Bell, K. J., 1966, "The Leidenfrost Phenomenon: Film Boiling of Liquid Droplets on a Flat Plate," *Int. J. Heat Mass Transfer*, Vol. 9, pp. 1167–1187.
- Grissom, W. M., and Wierum, F. A., 1981, "Liquid Spray Cooling of a Heated Surface," *Int. J. Heat Mass Transfer*, Vol. 24, pp. 261–271.
- Han, C. Y., and Griffith, P., 1965, "The Mechanism of Heat Transfer in Nucleate Pool Boiling—Part I," *Int. J. Heat Mass Transfer*, Vol. 8, pp. 887–904.
- Hiroyasu, H., Kadota, T., and Senda, T., 1974, "Droplet Evaporation on a Hot Surface in Pressurized and Heated Ambient Gas," *Bulletin of the JSME*, Vol. 17, pp. 1081–1087.
- Hosler, E. R., and Westwater, J. W., 1962, "Film Boiling on a Horizontal Plate," *ARS J.*, Vol. 32, pp. 553–558.
- Jeschar, R., Scholz, R., and Reiners, U., 1984, "Warmeübergang bei der zweiphasigen spritzwasserkühlung," *Gas-Warme Int.*, Vol. 33, p. 6.
- Klimenko, V. V., and Snytin, S. Y., 1990, "Film Boiling Crisis on a Submerged Heating Surface," *Exp. Thermal Fluid Sci.*, Vol. 3, pp. 467–479.
- Klinzing, W. P., Rozzi, J. C., and Mudawar, I., 1992, "Film and Transition Boiling Correlations for Quenching of Hot Surfaces with Water Sprays," *J. Heat Treating*, Vol. 9, pp. 91–103.
- Kovalev, S. A., 1966, "An Investigation of Minimum Heat Fluxes in Pool Boiling of Water," *Int. J. Heat Mass Transfer*, Vol. 9, pp. 1219–1226.
- Labeish, V. G., 1994, "Thermohydrodynamic Study of a Drop Impact Against a Heated Surface," *Exp. Thermal Fluid Sci.*, Vol. 8, pp. 181–194.
- Lienhard, J. H., 1976, "Correlation for the Limiting Liquid Superheat," *Chem. Eng. Sci.*, Vol. 31, pp. 847–849.
- Lienhard, J. H., and Karimi, A. H., 1978, "Corresponding States Correlations of the Extreme Liquid Superheat and Vapor Subcooling," *ASME JOURNAL OF HEAT TRANSFER*, Vol. 100, pp. 492–495.
- Matsuda, T., Taguchi, H., and Nagao, M., 1992, "Energetic Properties of NiO Surface Examined by Heat-of-Adsorption Measurement," *J. Thermal Analysis*, Vol. 38, pp. 1835–1845.
- McCann, H., Clarke, L. J., and Masters, A. P., 1989, "An Experimental Study of Vapor Growth at the Superheat Limit Temperature," *Int. J. Heat Mass Transfer*, Vol. 32, pp. 1077–1093.
- McCormick, J. L., and Westwater, J. W., 1965, "Nucleation Sites for Dropwise Condensation," *Chem. Eng. Sci.*, Vol. 20, pp. 1021–1036.
- Miller, C. A., and Neogi, P., 1985, *Interfacial Phenomena*, Marcel Dekker, New York.
- Nikolayev, G. P., Bychenkov, V. V., and Skripov, V. P., 1974, "Saturated Heat Transfer to Evaporating Droplets from a Hot Wall at Different Pressures," *Heat Transfer—Soviet Research*, Vol. 6, pp. 128–132.
- Nishio, S., and Hirata, M., 1978, "Direct Contact Phenomenon between a Liquid Droplet and High Temperature Solid Surface," *Sixth International Heat Transfer Conference*, Vol. 1, Toronto, Canada, Hemisphere, New York, pp. 245–250.
- Olek, S., Zvirin, Y., and Elias, E., 1988, "The Relation between the Rewetting Temperature and the Liquid-Solid Contact Angle," *Int. J. Heat Mass Transfer*, Vol. 31, pp. 898–902.
- Patel, B. M., and Bell, K. J., 1966, "The Leidenfrost Phenomenon for Extended Liquid Masses," *Chem. Eng. Progress Symposium Series*, Vol. 62, pp. 62–71.
- Ramilison, J. M., and Lienhard, J. H., 1987, "Transition Boiling Heat Transfer and the Film Transition Regime," *ASME JOURNAL OF HEAT TRANSFER*, Vol. 109, pp. 746–752.
- Rhodes, T. R., and Bell, K. J., 1978, "The Leidenfrost Phenomenon at Pressures up to the Critical," *Sixth International Heat Transfer Conference*, Vol. 1, Toronto, Canada, Hemisphere, New York, pp. 251–255.
- Sakurai, A., Shiotsu, M., and Hata, K., 1982, "Steady and Unsteady Film Boiling Heat Transfer at Subatmospheric and Elevated Pressures," *Heat Transfer in Nuclear Reactor Safety*, S. G. Bankoff and N. H. Afgan eds., Hemisphere New York, pp. 301–312.
- Schroeder-Richter, D., and Bartsch, G., 1990, "The Leidenfrost Phenomenon caused by a Thermo-Mechanical effect of Transition Boiling: A Revisited Problem of Non-Equilibrium Thermodynamics," *Fundamentals of Phase Change: Boiling and Condensation*, ASME, New York, pp. 13–20.
- Segev, A., and Bankoff, S. G., 1980, "The Role of Adsorption in Determining the Minimum Film Boiling Temperature," *Int. J. Heat Mass Transfer*, Vol. 23, pp. 637–642.
- Shepherd, J. E., and Sturtevant, B., 1982, "Rapid Evaporation at the Superheat Limit," *J. Fluid Mechanics*, Vol. 121, pp. 379–402.
- Skripov, V. P., 1974, *Metastable Liquids*, John Wiley and Sons, New York.
- Skripov, V. P., Sinityn, E. N., and Pavlov, P. A., 1980, *Thermal and Physical Properties of Liquids in the Metastable State*, Atomizdat, Moscow.
- Spiegler, P., Hopenfeld, J., Silberberg, M., Bumpus, Jr., C. F., and Norman, A., 1963, "Onset of Stable Film Boiling and the Foam Limit," *Int. J. Heat Mass Transfer*, Vol. 6, pp. 987–994.
- Taylor, G. I., 1950, "The Instability of Liquid Surfaces when Accelerated in a Direction Perpendicular to their Plane, I," *Proc. Royal Society of London*, Vol. A201, p. 192.
- Testa, P., and Nicotra, L., 1986, "Influence of Pressure on the Leidenfrost Temperature and on Extracted Heat Fluxes in the Transient Mode and Low Pressure," *Transactions of the ASME*, Vol. 108, pp. 916–921.
- Unal, C., Daw, V., and Nelson, R. A., 1992, "Unifying the Controlling Mechanisms for the Critical Heat Flux and Quenching: The Ability of Liquid to Contact the Hot Surface," *ASME JOURNAL OF HEAT TRANSFER*, Vol. 114, pp. 972–982.
- Xiong, T. Y., and Yeun, M. C., 1990, "Evaporation of a Liquid Droplet on a Hot Plate," *Int. J. Heat Mass Trans.*, Vol. 34, pp. 1881–1894.
- Yao, S. C., and Henry, R. E., 1978, "An Investigation of the Minimum Film Boiling Temperature on Horizontal Surfaces," *Transactions of the ASME*, Vol. 100, pp. 263–266.
- Yao, S. C., and Cai, K. Y., 1988, "The Dynamics and Leidenfrost Temperature of Drops Impacting on a Hot Surface at Small Angles," *Exp. Thermal Fluid Sci.*, Vol. 1, pp. 363–371.
- Zuber, N., 1958, "On the Stability of Boiling Heat Transfer," *Transactions of the ASME*, pp. 711–720.